EUROPEAN ORGANISATION FOR NUCLEAR RESEARCH

CERN PS DIVISION

CERN/PS 95-10 (DI)

RF TRAPPING AND ACCELERATION IN AUSTRON

E. Griesmayer[1]

Abstract

The rf trapping in the AUSTRON II and III machines is studied and optimized. Recommendations are made concerning chopping and momentum painting of the injected beam. In each case, the transverse tune shift and relative momentum spreads are calculated so that the risk of losses on non-linear resonances can be estimated and beam apertures calculated. This study is complementary to the main AUSTRON Feasibility Study for a fast-cycling, synchrotron-driven neutron spallation source.

Geneva, Switzerland
22 May 1995

[1] On leave of absence from the Atominstitut der Österreichischen Universitäten, Vienna, Austria

1. Introduction

Synchrotron-driven neutron spallation sources are space-charge limited and cycle with a frequency that is usually too high for the rf trapping to be fully adiabatic. In order to calculate efficient trapping and acceleration parameters in the synchrotron, it is necessary to use a tracking program that includes the space-charge effects [1]. The aim is always to reduce particle losses to an absolute minimum. This is necessary since the high repetition rate in this type of machine can cause serious deterioration of the equipment and make maintenance difficult due to the induced radioactivity caused by losses that would, in dc machines, be classed as minimal.

The study performed in this report is for the AUSTRON project [2] and calculates in detail the parameters and losses for AUSTRON II (25 Hz, 3.2×10^{13} protons per pulse) and AUSTRON III (50 Hz, 3.2×10^{13} protons per pulse). The aims are to keep particle losses as small as possible, the momentum spread of the particle distribution below 1.6 ‰ in order to avoid aperture problems and the transverse incoherent tune shift due to space charge below −0.35 in order to avoid crossing non-linear resonances.

2. General features

2.1 Stages of a cycle

The rf cycle can be conveniently divided into four parts, see also Figure 1:

(i) Trapping
Trapping includes a multi-turn, charge-exchange injection followed by a drift to the minimum magnetic field point. The period of charge-exchange injection is typically of the order of 100-200 turns and fills the machine to its nominal space-charge limit. This stage occurs on the downward slope of the magnetic field, a short time before the minimum is reached. The number of turns, the period of drift to the minimum of the field after injection and the profiles of the rf voltage and phase programmes are important parameters in the cycle. During the injection and drift to the minimum field, the rf bucket is stationary and its equilibrium orbit drifts outwards to the central orbit. This is an important feature in the painting of the transverse phase space, which is described in [2].

(ii) Acceleration to the *first critical point*
From the minimum of the magnetic field, the rf bucket starts to accelerate keeping the beam centred in the vacuum chamber. The profile of the rise of the rf voltage is an important factor in maintaining the bucket area during this period. Shortly after the minimum field, typically 2 ms in AUSTRON II and 1 ms in AUSTRON III, the first critical point occurs. At this point, the momentum spread reaches its maximum and an aperture limitation occurs.

(iii) Acceleration to *second critical point*
After the first critical point the magnetic field rises more rapidly and in a 25 or 50 Hz machine the demands on the rf are high. Since rf voltage is limited in the AUSTRON by space and cost (as would probably be the case in most machines), it is necessary to

allow the synchronous phase to increase considerably. Even with full rf voltage applied this has the immediate effect of reducing the bucket size and considerable losses can occur up to about the middle of the cycle when the rate of field change and the synchronous phase are maximum. This is the second critical point when the synchronous phase becomes biggest and the bunch width is therefore a minimum.

(iv) Acceleration to the final energy where the beam is extracted.
Once the rate of field change decreases in the second half of the cycle, the synchronous phase reduces and the beam becomes small with respect to the bucket.

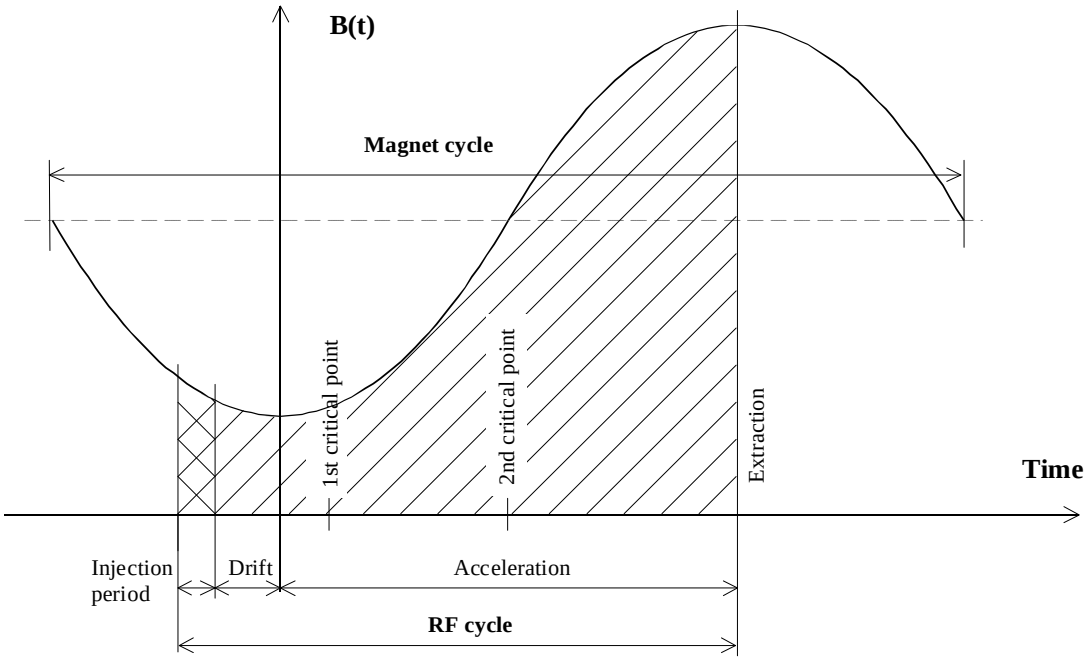

Figure 1 Magnetic field and the stages of an rf cycle

2.2 Losses

Losses occur when particles, which are outside the rf bucket, reach a momentum deviation with respect to the synchronous particle that is larger than the momentum acceptance of the machine. There are two types of particle losses, the *trapping losses* and the *acceleration losses.* Trapping losses occur up to the first critical point when particles that fall outside the rf bucket during the injection and drift periods get lost as the beam started to accelerate. Acceleration losses occur between the first and the second critical point because the rf bucket shrinks during acceleration and particles close to the separatrix leave the bucket. Acceleration losses happen at higher energies than trapping losses and are therefore potentially more dangerous from an irradiation point of view. After the second critical point, there will be no further losses.

Losses can be minimized by optimizing the rf program and the timing of the injection period and the drift time. In addition to this, the overall losses can be influenced by *chopping* the beam and by *momentum painting* the beam. Chopping is carried out at a

far lower energy where losses cause little or no induced activity. The chopped beam is effectively a pre-bunched beam which is synchronized with the rf bucket. Momentum painting can be achieved by modulating the debunching cavity during the injection time. Momentum painting provides a way of influencing the uniformity of the filling of the rf bucket.

3. Trapping and acceleration in AUSTRON

AUSTRON general parameters:

(a) Machine parameters:

Injection energy	W = 130 MeV
Extraction energy	W = 1.6 GeV
Average machine radius	R = 33.9 m
Bending radius	ρ = 8.346 m
Transition energy	γ_t = 4.25
Harmonic number	h = 2
Chamber size/beam size	b/a = 1.1
Magnet field	$B(t) = B_0 - B_1\cos(2\pi ft)$
where	B_0 = 0.5734 T and B_1 = 0.3692 T
Transverse tune	Q_x = 4.25, Q_y = 4.20

(b) Beam parameters:

Parabolic momentum distribution,
Total relative momentum spread $\Delta p/p = \pm 2$ ‰,
Phase spread from $-\pi$ to $+\pi$,
Total number of protons per pulse $N = 3.2\text{x}10^{13}$,
Macro particles used for the calculations N_{mp} = 12’600,
Injection time interval started at –440 μs and lasting over 200 μs.

4. The trapping and acceleration cycle in AUSTRON II

AUSTRON II operates at 25 Hz. The rf cycle therefore lasts from the beginning of the injection to 20 ms, the equivalent to half a magnet cycle.

4.1 The rf program

Figure 2 shows an optimized rf voltage program for AUSTRON II. The initial voltage is increased slowly from 0 kV to 5 kV during injection and to 20 kV during the drift period. The maximum voltage is 160 kV and the maximum synchronous phase is 40 deg.

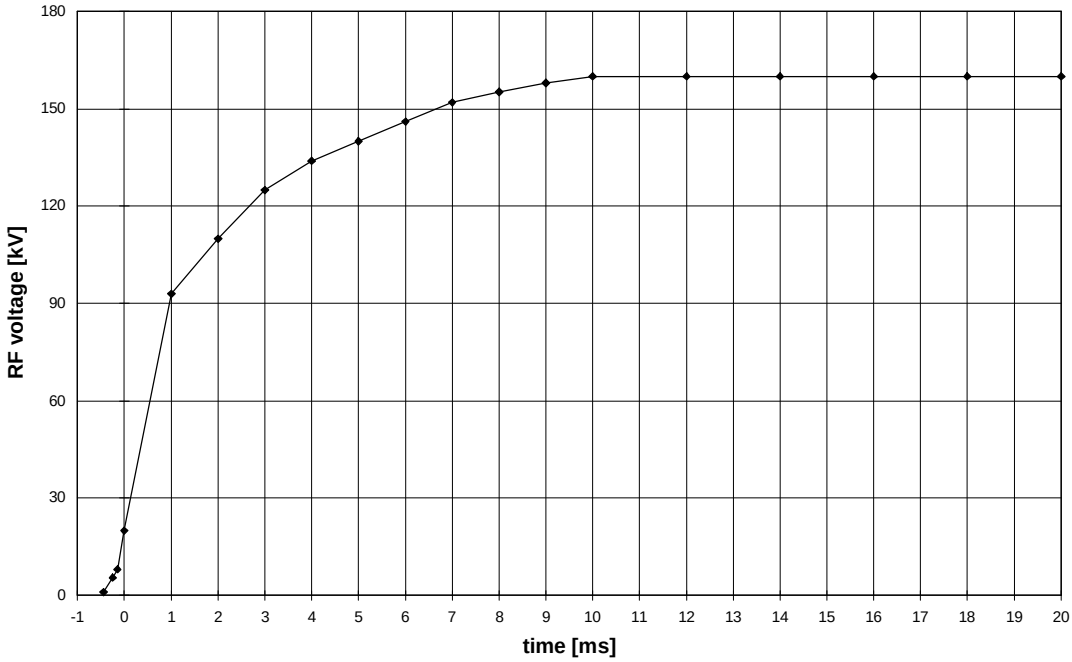

Figure 2 The rf voltage program for AUSTRON II

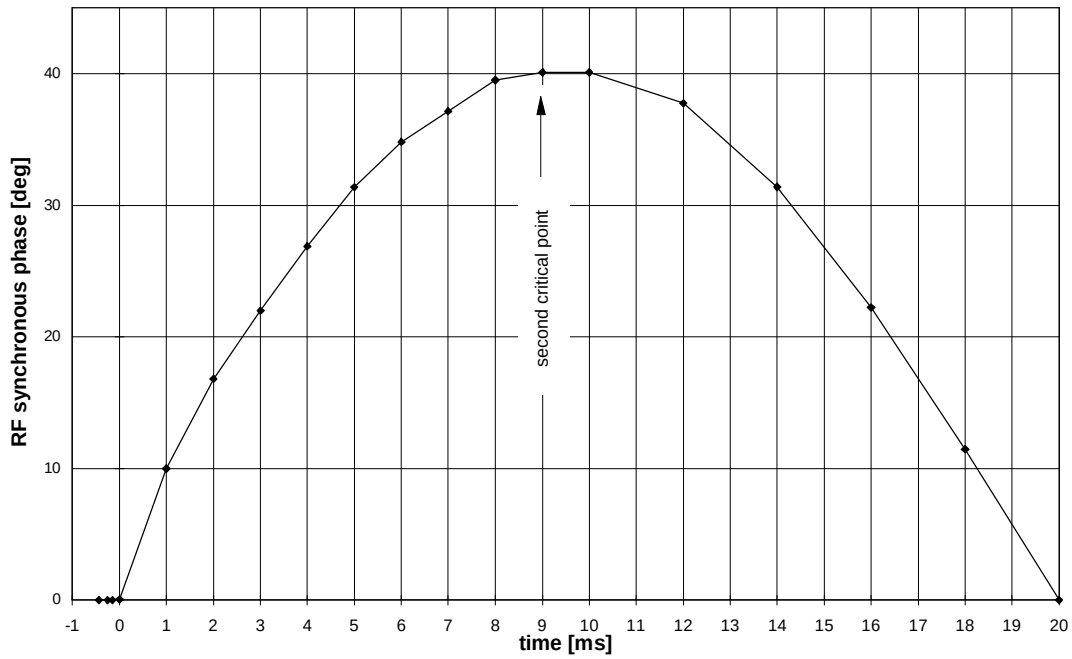

Figure 3 The synchronous phase variation for AUSTRON II

For AUSTRON II, the optimization has been made so that the first beam injected rotates by about 4 rad in the longitudinal phase plane once the minimum field point has been reached. The form of the rf voltage is also optimized to achieve the lowest losses. After the minimum field point, acceleration starts and it is necessary to apply the rf voltage in such a way that the synchronous phase increases smoothly. Between the field minimum and the first critical point there is a subtle balance between losses and the maximum momentum spread. Too much voltage will give a too larger momentum spread and a smaller voltage will not provide the wanted beam rotation. After the first critical point the voltage increases further, but again it is necessary to

keep the change of the synchronous phase smooth. Otherwise there are rapid changes in the positions of the separatrices and particles can 'jump' out of the bucket. Figure 3 shows the evolution of the synchronous phase.

4.2 Momentum spread and transverse tune shift in AUSTRON II

The total relative momentum spread increases from the initial value of 0.4 % to its maximum at the first critical point, which appears at about 2 ms. The solid line in Figure 4 shows the total relative momentum spread of all particles, which peaks at 3.6 %. This big momentum spread is caused by a few particles which have already left the rf bucket and will be lost on a momentum collimator. Only the core particles will survive and the dotted line indicates their momentum spread and its maximum of about 1.8 %.

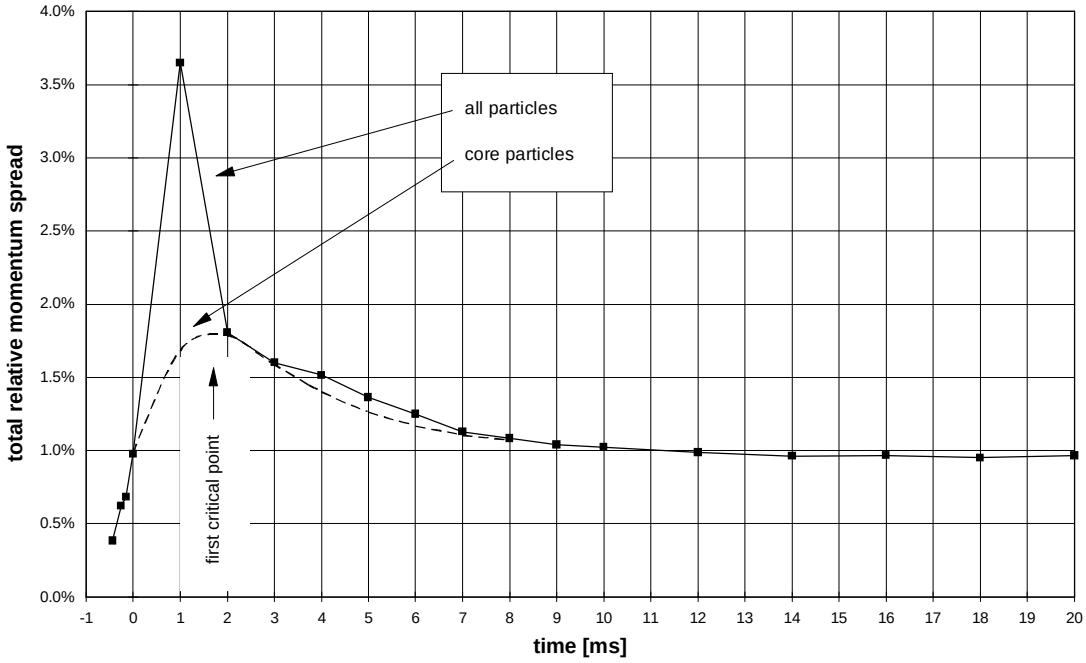

Figure 4 The total relative momentum spread during the rf cycle in AUSTRON II

Figure 5 shows that the incoherent betatron tune shift crosses the limit of −0.35 for less than 1 ms and that it stays above −0.4, which seems to be tolerable.

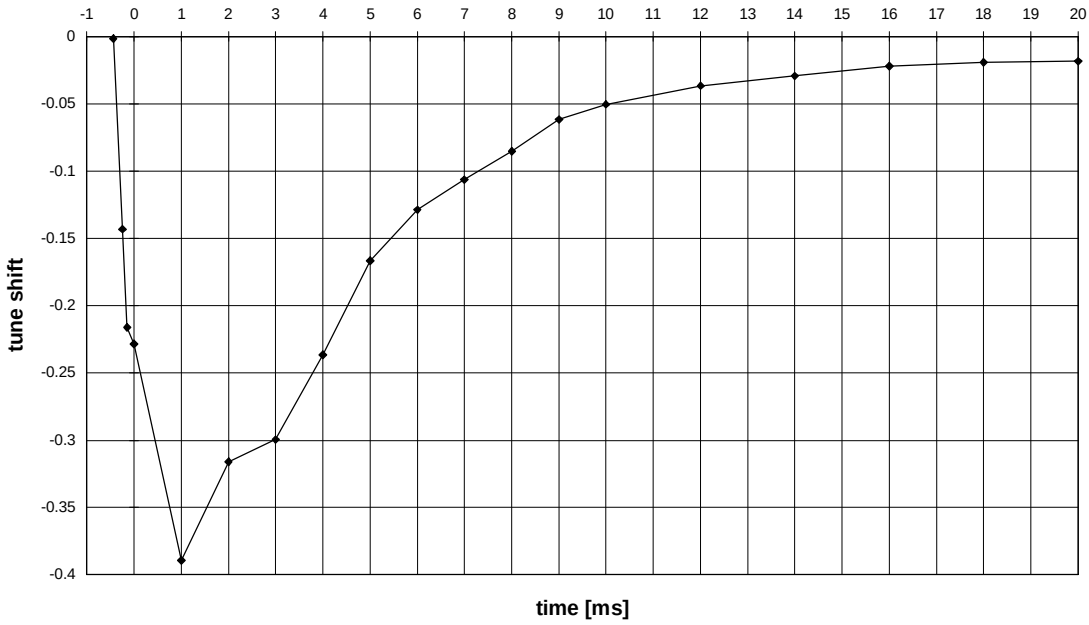

Figure 5 The incoherent betatron tune shift during the rf cycle in AUSTRON II

4.3 Losses in AUSTRON II

The loss distribution is shown in Figure 6. The total loss is 0.4 %, whereof 42 % are trapping losses and the rest acceleration losses. The first critical point appears at about 2 ms and the second critical point at about 8 ms.

4.4 Summary for AUSTRON II

It appears unnecessary to employ the complicated techniques of chopping and/or momentum painting in AUSTRON II. It is therefore proposed that AUSTRON II is constructed with a continuous beam of 128 μA average current, without chopper and a total momentum spread from the linear accelerator of ±2 ‰. This is not very demanding for the debuncher. With the system proposed in [2] the voltage on the debunching cavity could be reduced from 1.2 MV to about 0.6 MV. This and the required H^- source are within the current technologies.

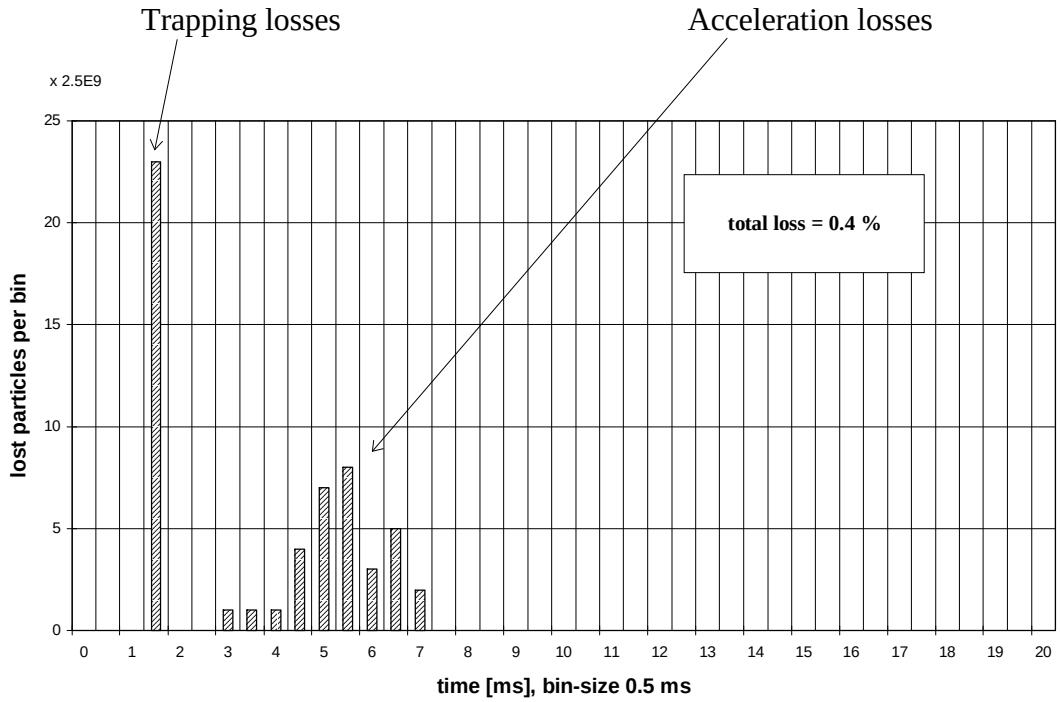

Figure 6 Beam losses during the rf cycle in AUSTRON II

5. The trapping and acceleration cycle in AUSTRON III

5.1 The rf program

AUSTRON III operates at 50 Hz. The rf cycle lasts from the beginning of the injection to 10 ms. In AUSTRON III the acceleration is faster compared to AUSTRON II by a factor of two which leads to higher rf voltage requirements and to higher losses. Figure 7 shows the rf voltage program for AUSTRON III which was optimized such that the trapping losses and the acceleration losses are minimized. The voltage increases linearly from zero to 5 kV during injection and on to 20 kV during the drift to the minimal field point. Then it increases and peaks at 5 ms at 246 kV. This allows the rf synchronous phase, which is shown in Figure 8, to increase as smoothly as possible and leads to minimized acceleration losses. The maximum rf synchronous phase is 64.8 deg.

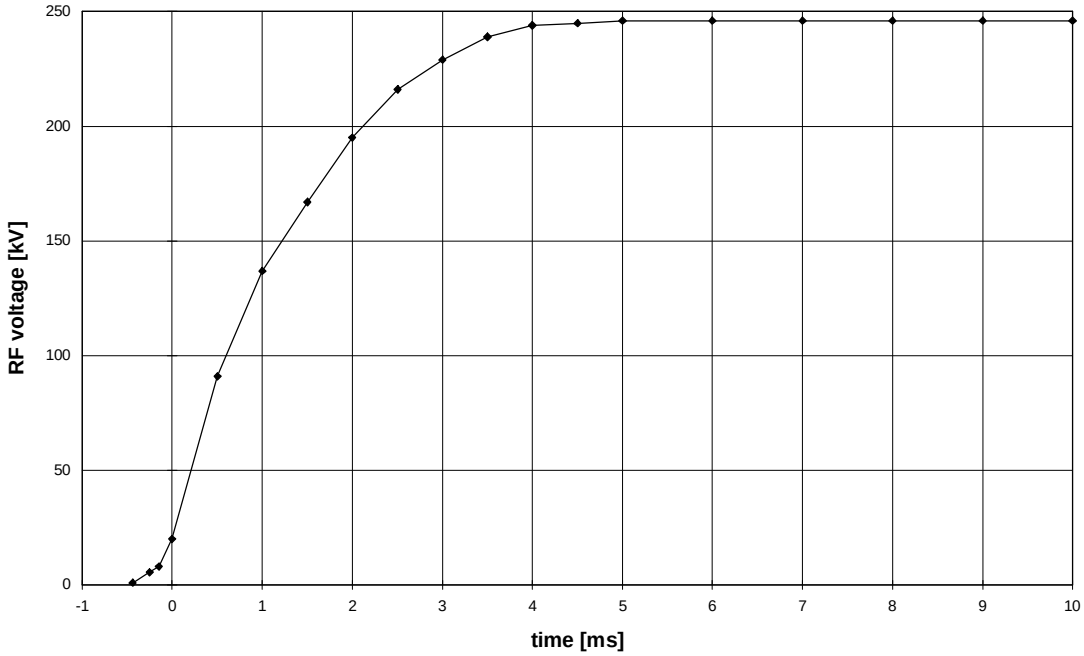

Figure 7 The rf voltage program for AUSTRON III

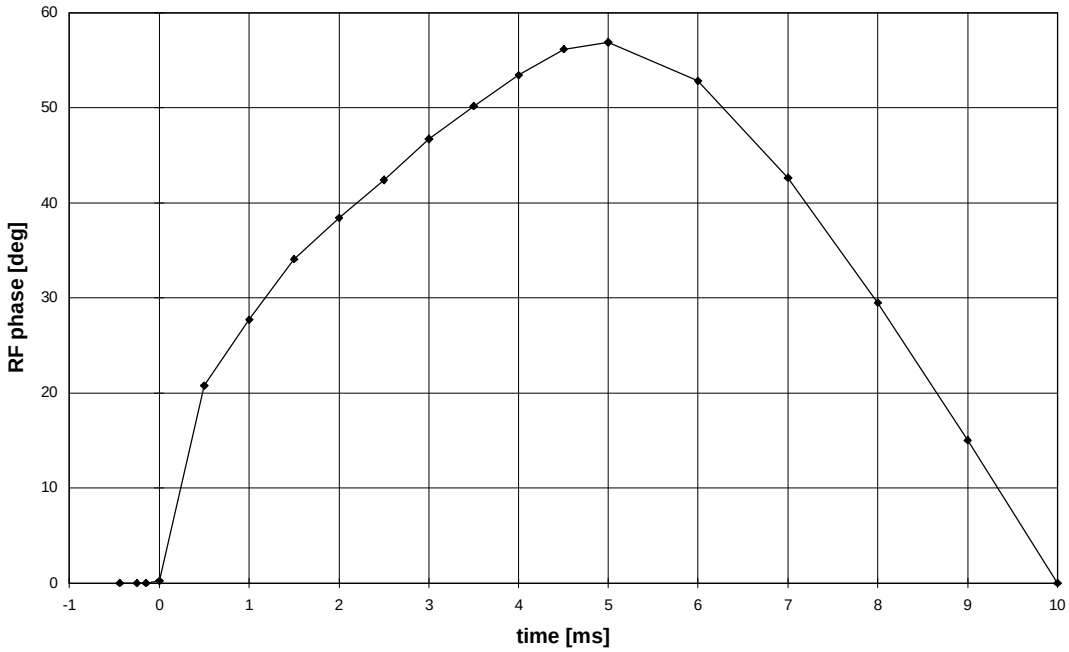

Figure 8 The synchronous phase variation for AUSTRON III

5.2 Momentum spread and transverse tune shift in AUSTRON III

The total relative momentum spread for AUSTRON III is shown in Figure 9. The maximum momentum spread of the core particles is less than 1.7 % and appears at the first critical point at 1 ms. The maximum momentum spread of all particles peaks at 3.5 %, which is caused by the few particles that have already left the rf bucket and will be lost at a later time on the momentum collimator. Only the core of the bunch will survive.

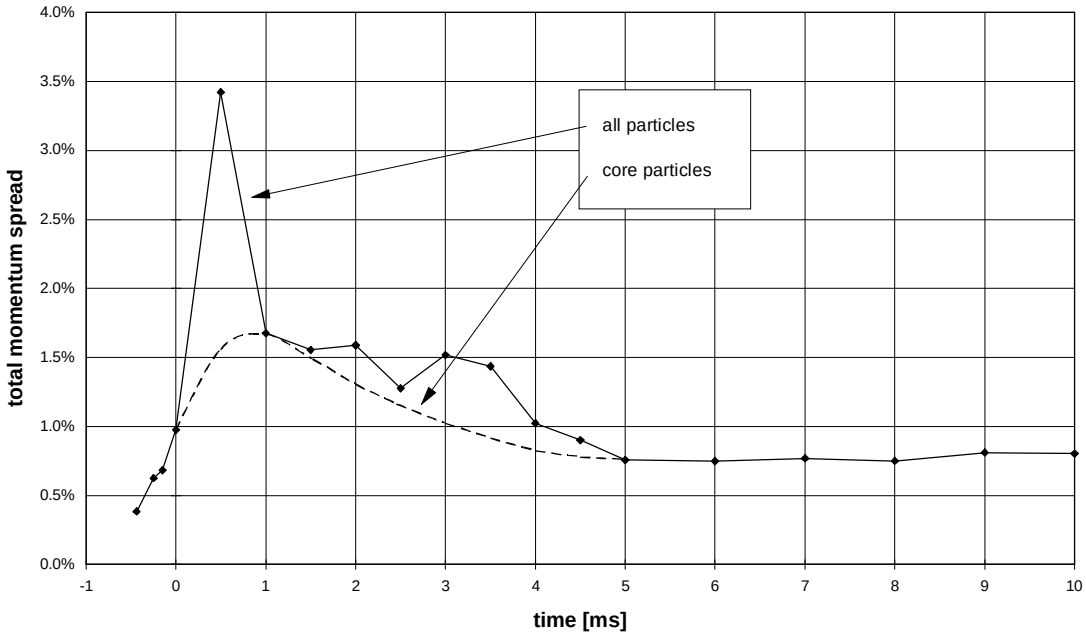

Figure 9 The total relative momentum spread during the rf cycle in AUSTRON III

The incoherent betatron tune shift due to space charge is shown in Figure 10. The maximum tune shift is less than –0.35, and is therefore within the tolerance.

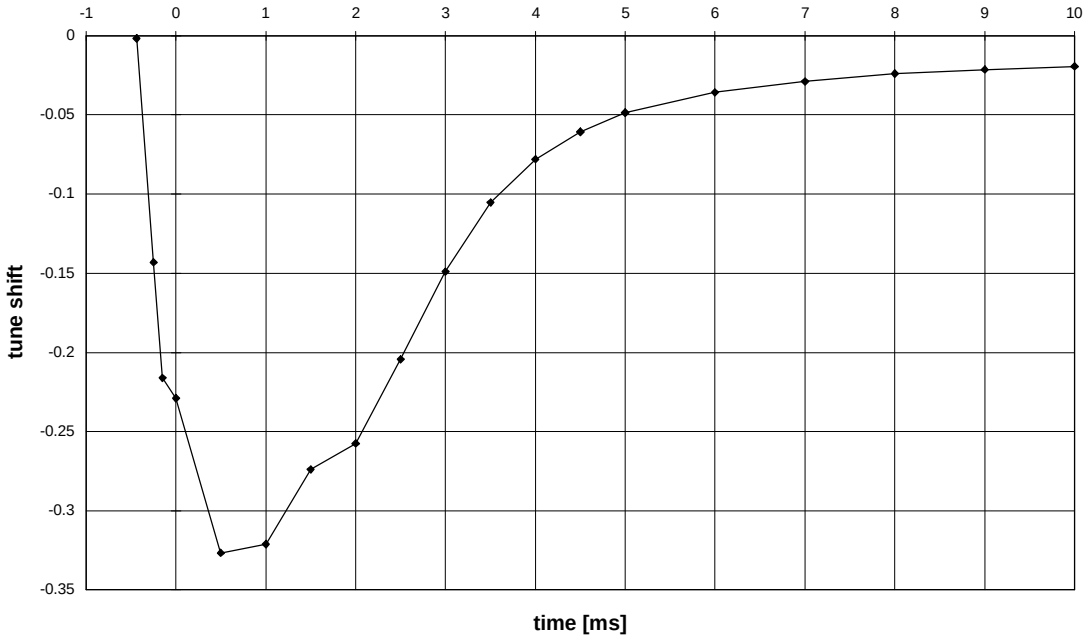

Figure 10 The incoherent betatron tune shift during the rf cycle in AUSTRON III

5.3 Losses in AUSTRON III

In the case of AUSTRON III the losses for a coasting beam agree with the assumptions made in [2] i.e. 10 %, as shown in Figure 11. It should also be noted that

the majority of the losses are acceleration losses (90%) and therefore occur at a higher energies and consequently cause more induced activity. For this reason, the use of a chopper has been investigated.

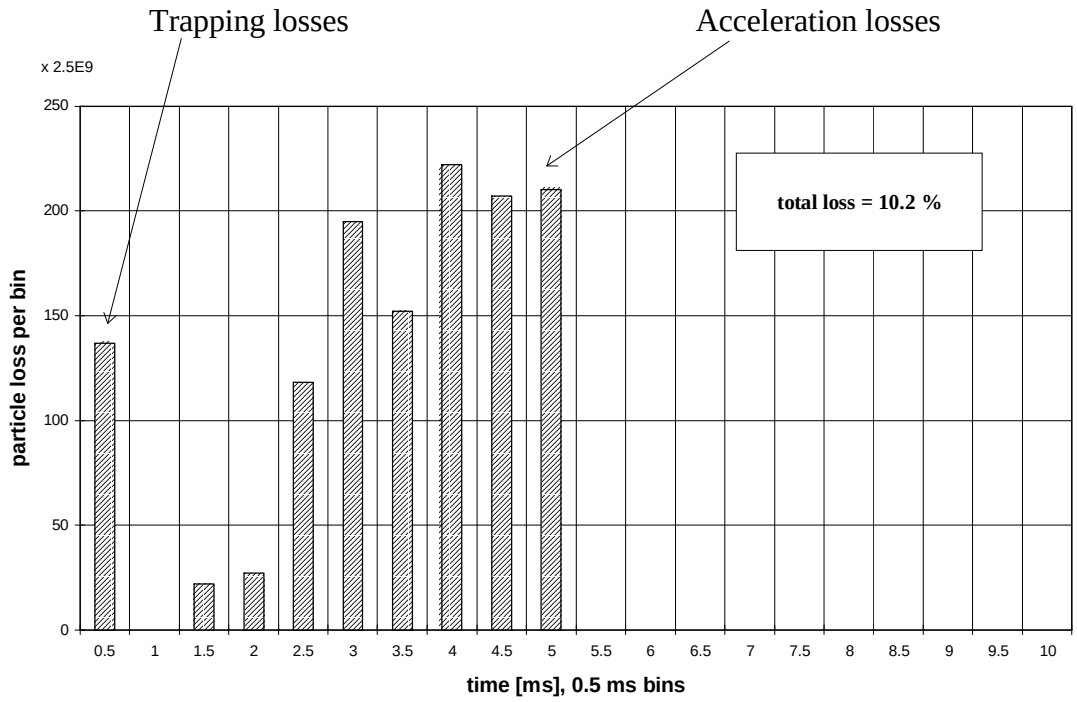

Figure 11 Beam losses during the rf cycle in AUSTRON III

5.4 Chopping

Figure 12 shows how the losses vary with the percentage chopping. It should be noted that chopping increases the requirements on the current source, which for AUSTRON III is already beyond the limit of current technology. However, there may be the possibility of designing the injection bump in such a way that the injection period can be increased and hence the current requirement reduced. Figure 12 shows that chopping at up to 50 % seems to be advantageous for AUSTRONIII when considering only trapping and acceleration losses. Chopping does however increase the betatron tune shift, as shown in Figure 13, which could increase the losses on non-linear resonances but the net result is probably in favour of chopping.

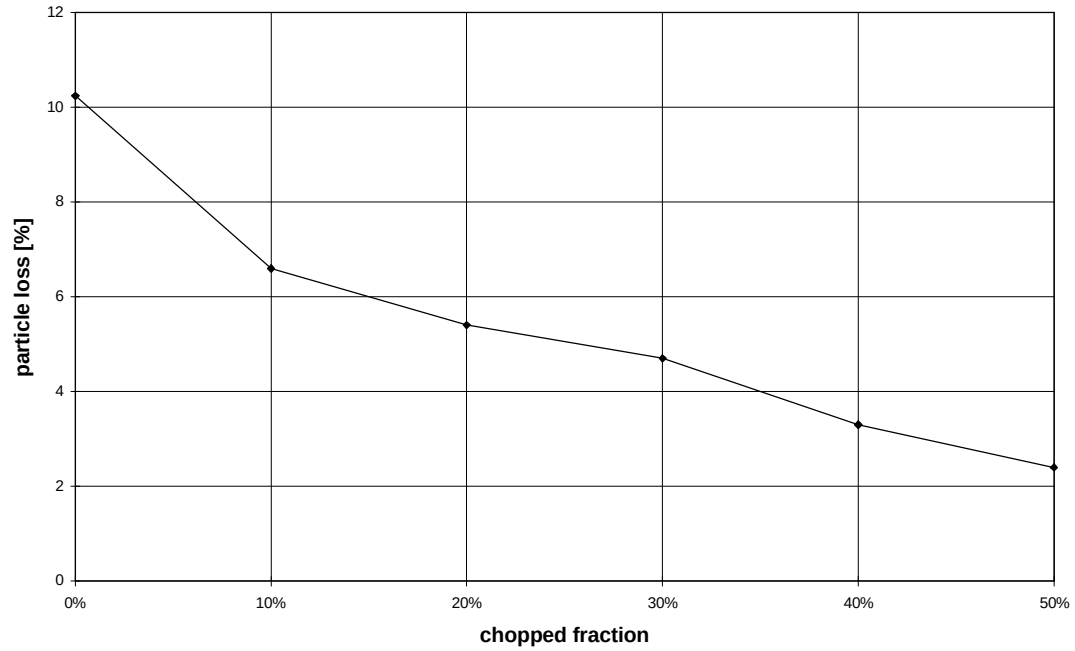

Figure 12 Variation of losses with chopping in AUSTRON III

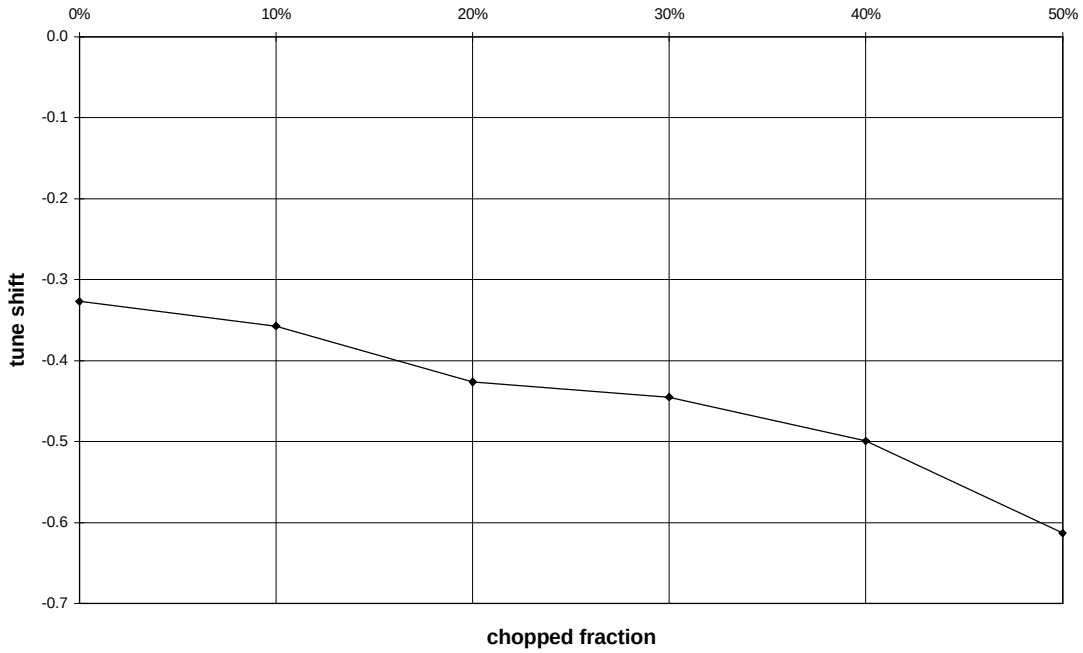

Figure 13 Variation of incoherent betatron tune shift with chopping in AUSTRON III

5.5 Momentum painting

Momentum painting is another technique which can potentially reduce losses. The aim here is to obtain a smoother distribution in the bucket for the injected beam[2]. This can

[2] Momentum painting can also be used to paint in the transverse plane by injecting in a dispersive region. In the AUSTRON transverse painting is assured by the falling field and a fast bump.

be done by sweeping the momentum of the injected beam by means of the debunching cavity. Typically the painting would be from -1 to +1 ‰ or -2 to +2 ‰ with a narrow beam of ±1 ‰ or less. Table 1 compares these two cases with static beams of ±1 ‰ and ±2 ‰ total momentum spread.
Momentum painting a pencil beam of +1 ‰ over the ranges -1 ‰ to +1 ‰ and -2 ‰ to +2 ‰ gives losses in the order of 8 % which is slightly better than injecting a beam of ±2 ‰ directly. However, if a debunching cavity is present the losses are reduced further to 6.8 % by simply injecting the ±1 ‰ beam without any painting. The indication is that if a high performance debunching cavity is available it may be better to use it without painting.

Initial momentum spread [‰]	Painting range [‰]	Loss [%]	Maximum incoherent tune shift
±1	–1 to +1	8.2	–0.41
±1	–2 to +2	8.3	–0.48
±1	none	6.8	–0.51
±2	none	10.2	–0.33

Table 1 Momentum painting in AUSTRON III

5.6 Summary for AUSTRON III

However, there is no clear advantage in painting a ±1 ‰ beam compared to the static ±2 ‰ beam in AUSTRON III, as the reduction of losses is accompanied by an increased transverse tune shift which may well cause the same or greater losses on non-linear resonances. The case for high performance debunching cavities for AUSTRON III is not adequately justified by these results. Chopping at up to 50 % appears very advantageous, but increases the current requirements of the source and the effects of space charge.

6. Future prospects

6.1 Increased rf voltage in AUSTRON III

The increase of acceleration losses with respect to trapping losses in AUSTRON III indicates that more rf voltage is needed. However there is no space available in the AUSTRON ring for additional cavities. This implies that either an improved cavity design is needed or the ring should be increased in size.

6.2 Possible upgrade to 0.5 MW

All machines show a performance improvement with time and it is hoped that the space charge limits of AUSTRON III could be raised by accepting a larger incoherent tune shift. This might be achieved by the installation of a resonance compensation scheme. In preparation for this improvement, Table 2 shows the losses, if beam intensities are increased from the design 0.41 MW beam by about 25 % to deliver

0.5 MW to the target and where chopping has been included. The losses increase by about 20 % and the transverse tune shift increases much more dramatically.

Chopped fraction [%]	Loss [%]	Maximum incoherent tune shift
0	9.2	–0.46
10	6.8	–0.54
20	6.6	–0.55
30	5.2	–0.57
40	4.5	–0.66
50	4.4	–0.69

Table 1 Loss and transverse tune shift in the case of 0.5 MW

7. Conclusion

In the case of AUSTRON II, a continuous non-chopped beam with a relative total momentum spread of ±2 ‰ causes particle losses of 0.4 %, which is considerably less than the assumed 10 % in [2]. This gives confidence that the irradiation in AUSTRON II will be well under control.

In AUSTRON III a pencil beam leads to total losses of 10.2 %. By chopping these losses can be reduced to about 2 %, but this reduction is accompanied by an increased transverse tune shift. However, it may be possible to avoid the disadvantage of the larger tune shift by compensating one or more non-linear resonances. It should be noted that chopping implies either a higher performance current source, or a redesign of the injection bump. In the case of AUSTRON, momentum painting of the beam does not seem to be worthwhile

8. Acknowledgements

This work was performed at CERN within the framework of the AUSTRON Feasibility Study.that was commissioned and supported by the Austrian Government and hosted by CERN. In particular, I should like to thank the PS Division in CERN for their hospitality. I should also like to acknowledge the help of Shane Koscielniak, who adapted his computer code (LONG1D) for the requirements of AUSTRON,. and to thank Horst Schönauer, Kjell Johnsen and Phil Bryant for their advice and help.

9. References

[1] S.R. Koscielniak, '*LONG1D Users Guide*', TRIUMF Design Note, TRI-DN-88-20, May 1988

[2] P.J. Bryant et al., '*AUSTRON Feasibility Study*', (AUSTRON Planning Office, c/o Atominstitut der Österreichischen Universitäten, Vienna), November 1994, also to be published as a CERN Divsional Report.

Appendix A

Results from Program LONG1D [1] for AUSTRON II

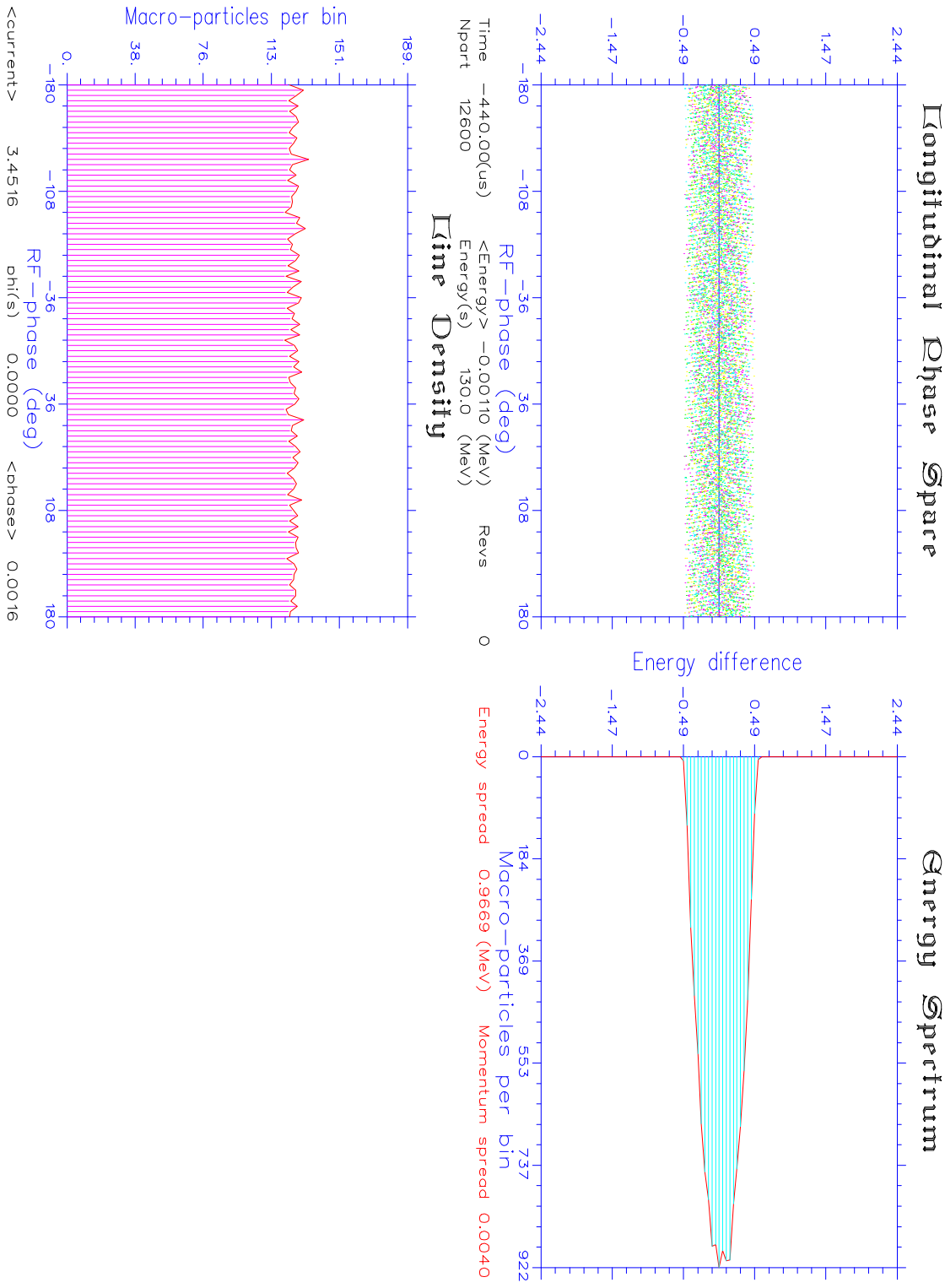

Figure A1 The initial beam distribution with a coasting beam with $\Delta p/p = \pm 2$ ‰

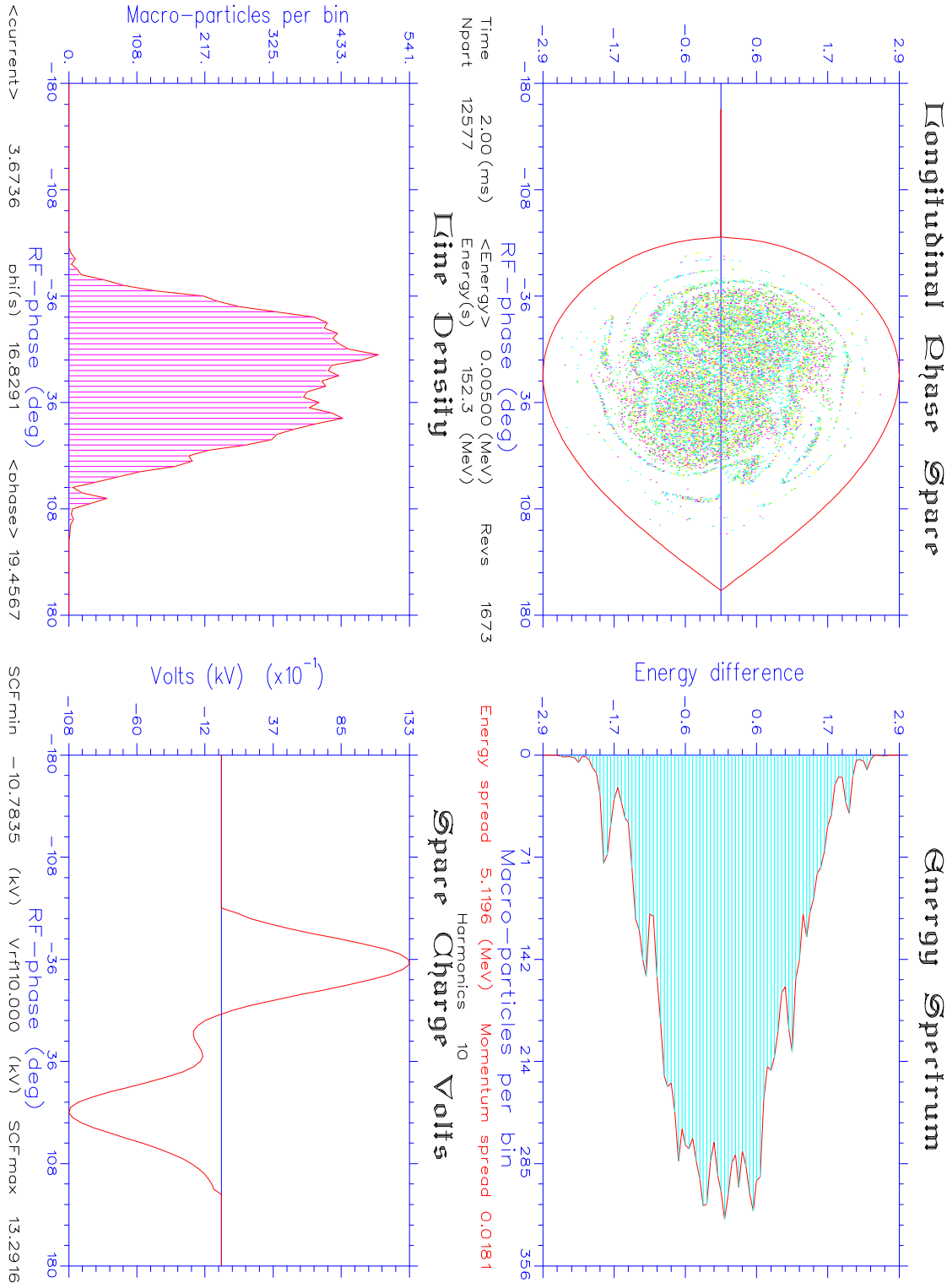

Figure A2 Beam distribution for AUSTRON II at the *first critical point* at 2 ms, where $\Delta p/p$ reaches its maximum

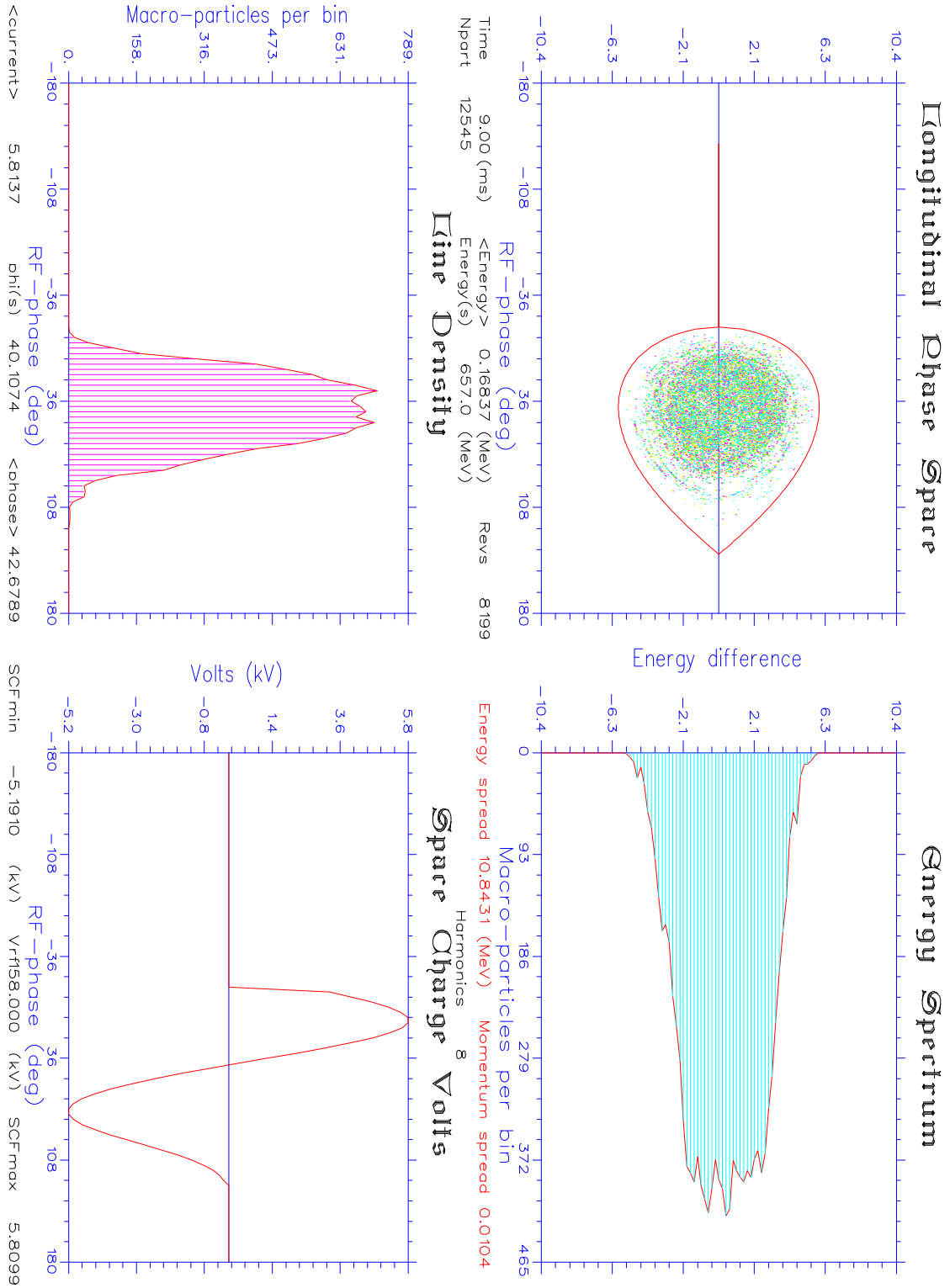

Figure A3 Beam distribution for AUSTRON II at the *second critical point* at 9 ms, where the synchronous phase reaches its maximum and where the bunch is smallest

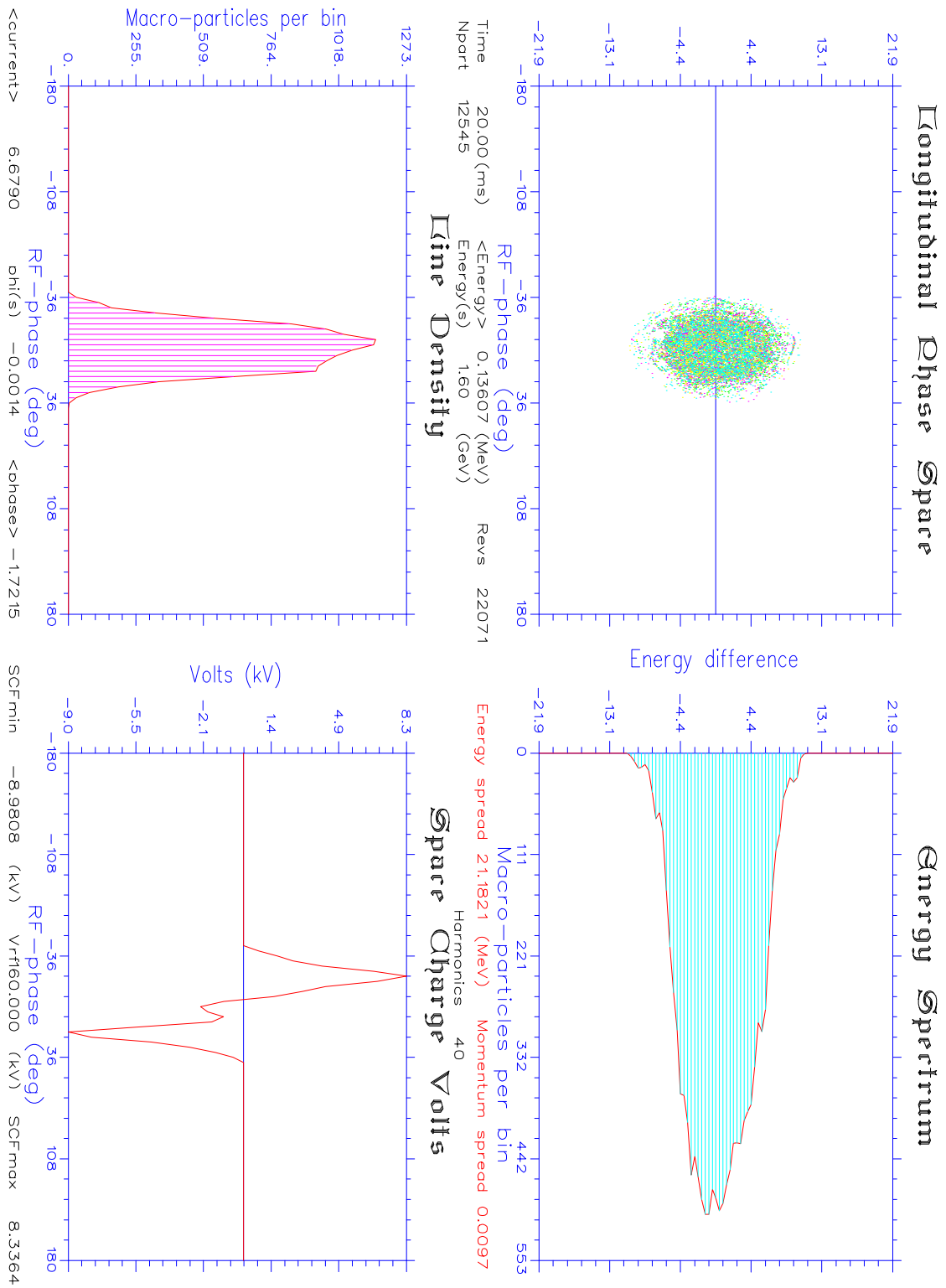

Figure A4 Beam distribution of AUSTRON II at the extraction at 20 ms. The separatrix is not shown, but the rf bucket is much larger than the beam.

Appendix B

Results from Program LONG1D [1] for AUSTRON III

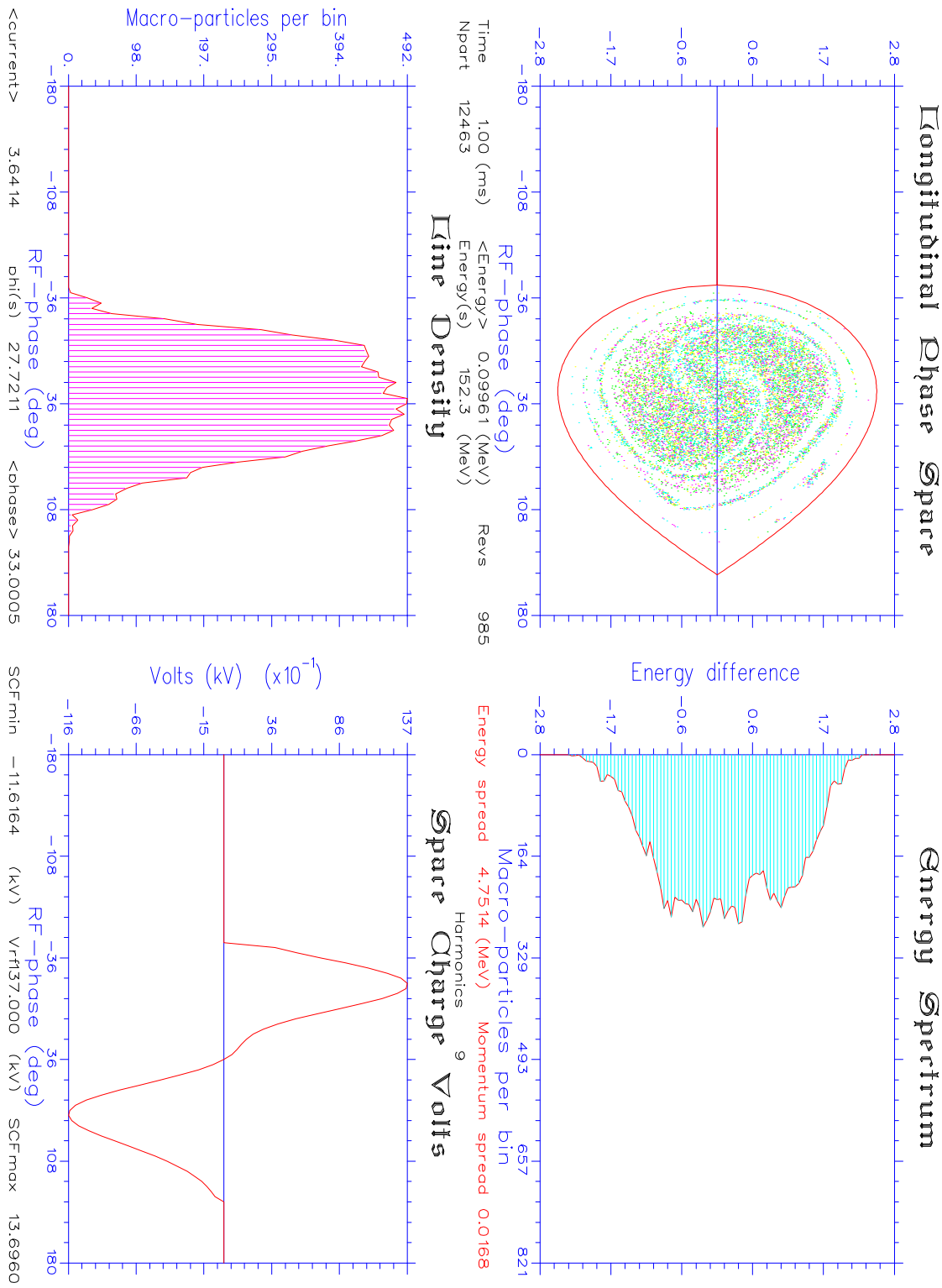

Figure B1 Beam distribution for AUSTRON III at the *first critical point* at 1 ms, where $\Delta p/p$ reaches its maximum

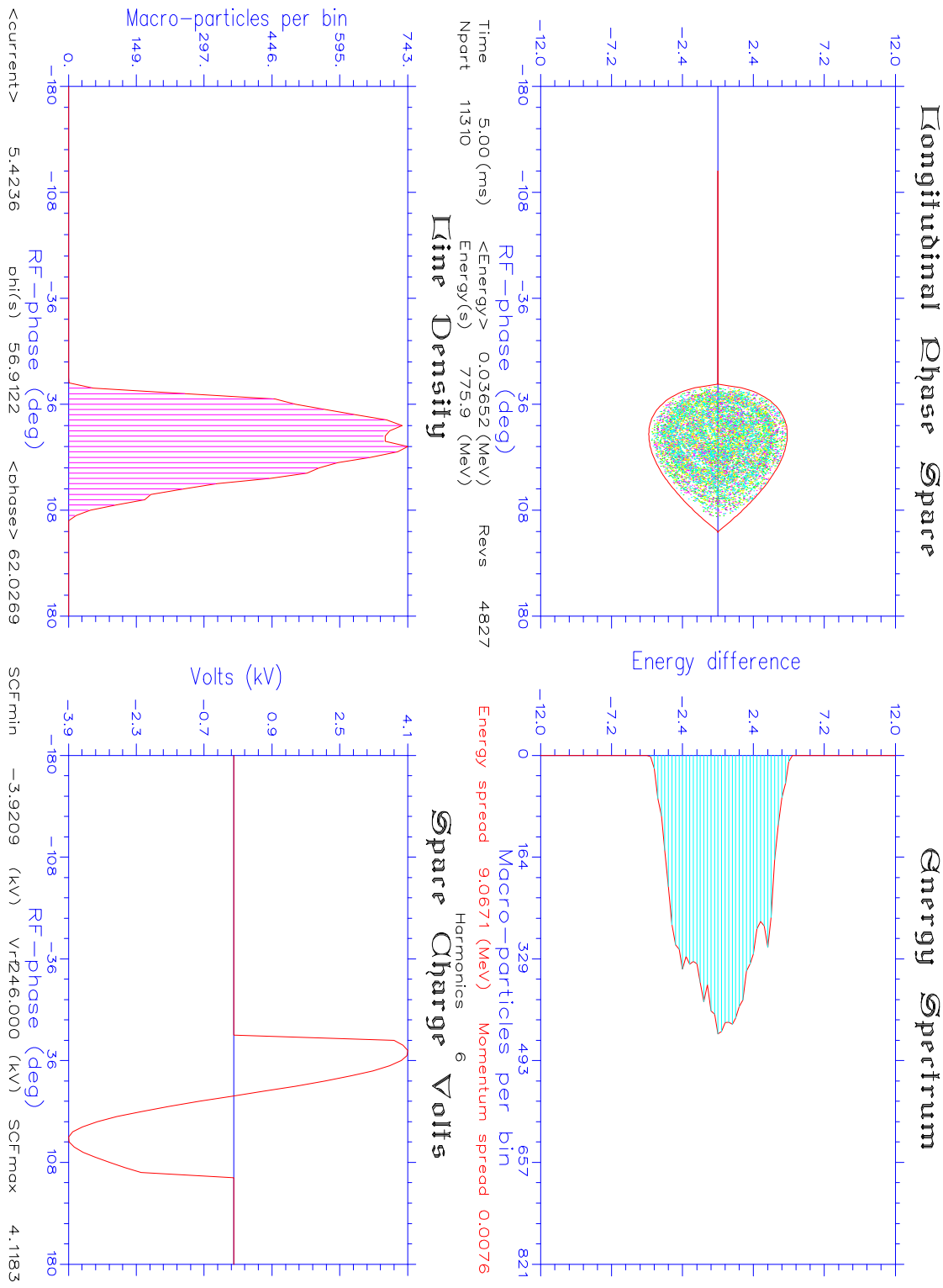

Figure B2 Beam distribution for AUSTRON III at the *second critical point* at 5 ms, where the synchronous phase reaches its maximum and where the bunch is smallest

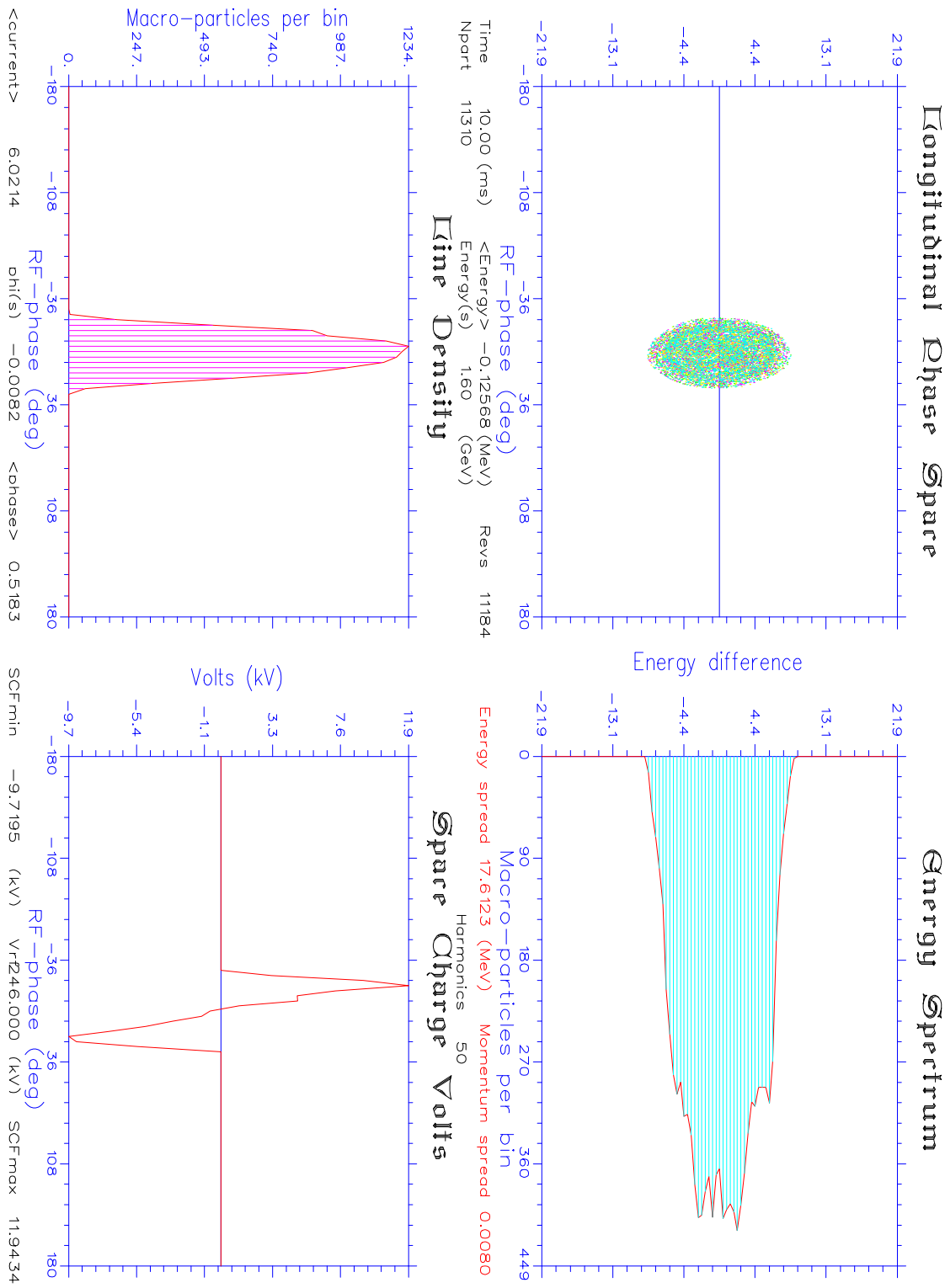

Figure B3 Beam distribution for AUSTRON III at the extraction at 10 ms. The separatrix is not shown, but the rf bucket is much larger than the beam.

* * *